# Low-energy electron microscopy of graphene outside UHV: electron-induced removal of PMMA residues used for graphene transfer

E. Materna Mikmeková[a,*], I. Müllerová[a], L. Frank[a], A. Paták[a], J. Polčák[b,c], S. Sluyterman[d], M. Lejeune[e], I. Konvalina[a]

[a] The Czech Academy of Sciences, Institute of Scientific Instruments, Královopolská 147, 612 64 Brno, Czech Republic
[b] Institute of Physical Engineering, Brno University of Technology, Technická 2896/2, 616 69 Brno, Czech Republic
[c] CEITEC - Central European Institute of Technology, Brno University of Technology, Purkyňova 123, 612 00 Brno, Czech Republic
[d] FEI/ThermoFisher Scientific, Achtseweg Noord 5, 5651 GG Eindhoven, the Netherlands
[e] Laboratoire de Physique de la Matière Condensée, Université de Picardie Jules Verne, 33 rue Saint Leu, 80039 Amiens, France

## ARTICLE INFO

## ABSTRACT

Two-dimensional materials, such as graphene, are usually prepared by chemical vapor deposition (CVD) on selected substrates, and their transfer is completed with a supporting layer, mostly polymethyl methacrylate (PMMA). Indeed, the PMMA has to be removed precisely to obtain the predicted superior properties of graphene after the transfer process. We demonstrate a new and effective technique to achieve a polymer-free CVD graphene — by utilizing low-energy electron irradiation in a scanning low-energy electron microscope (SLEEM). The influence of electron-landing energy on cleaning efficiency and graphene quality was observed by SLEEM, Raman spectroscopy (the presence of disorder D peak) and XPS (the deconvolution of the C 1s peak). After removing the absorbed molecules and polymer residues from the graphene surface with slow electrons, the individual graphene layers can also be distinguished outside ultra-high vacuum conditions in both the reflected and transmitted modes of a scanning low-energy (transmission) electron microscope.

## 1. Introduction

Two dimensional materials, such as graphene, have attracted significant interest because of their unique electrical, mechanical, and optical properties. They, therefore, have a potential use in various fields, such as field-effect transistors (FETs), sensors, integrated electronic circuits, large-scale transparent electrodes, and opto-electronics. [1–12]

Nowadays, the CVD technique (Chemical Vapor Deposition) is the most reliable synthesis method because of the industrial-scale production of cheap and high-quality graphene. [13] On the other hand, for applications of CVD-grown graphene, this atomically thin film has to be exfoliated and transferred to selected substrates. This is typically performed with a supporting layer, such as polymethyl methacrylate (PMMA), and, after the transfer process, the PMMA is usually removed by an organic solvent — acetone. However, because of the strong interaction between PMMA and the deposited material, its residue is left on the surface. This leads to significant contamination of the graphene. [14,15] In this paper, the multi-layered graphene was deposited by CVD technique. Chemical exfoliation, which uses PMMA film, was used for

preparation of the free-standing samples. It should be noted, that direct transfer of graphene layers based on surface tension draws was already described. [16] Unfortunately, the method described above includes chemicals (isopropanol), which is also significant source of contamination, especially in electron microscopy: it creates amorphous carbon-based film under electron beam. The following cleaning of the samples prepared by the direct transfer was realized by heating (in/outside a vacuum) [17] or by dry cleaning with adsorbents [18] and tested in transmission electron microscopes (TEMs). Nevertheless, only the small graphene flakes can be prepared by the direct transfer. From practical point of view, the usage of PMMA during the exfoliation process is the best verification method at the moment.

Indeed, the development of new types of material, such as 2D crystals, requires the emergence of new surface-sensitive techniques for their characterization. With regards to the "surface" sensitivity, ultra-low-energy electron microscopy can be a very powerful tool for the true examination of these atom-thin materials that are capable of confirming the physical phenomena predicted to occur on their surfaces. Modern commercial scanning electron microscopes enable imaging and analyses with low-energy electrons, even at very high magnification. In the
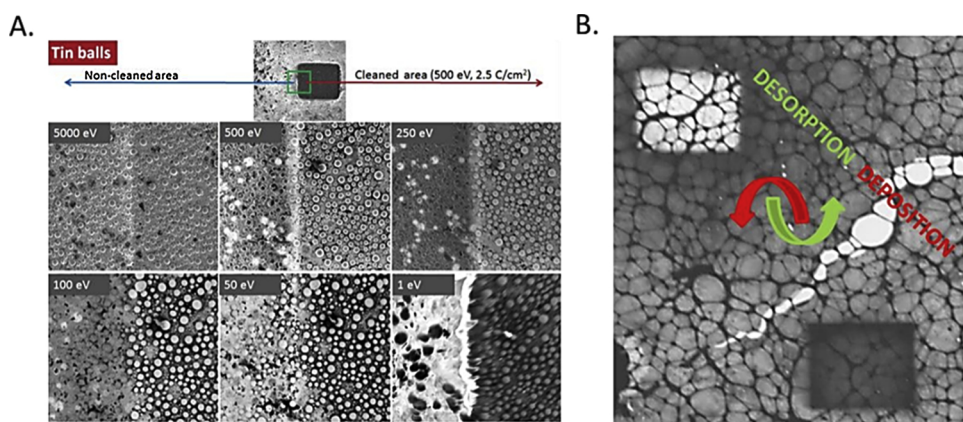
---

**Fig. 1.** (A) Tin balls observed with 5000 eV, 500 eV, 250 eV, 100 eV, 50 eV, and 1 eV electrons (the left half of each frame shows the non-cleaned area covered with adsorbed molecules, while the right half is the area cleaned by slow electrons); (B) Low voltage STEM observation at 100 eV of graphene after irradiation by electrons that caused deposition (irradiation by 5 keV) and desorption (irradiation by 500 eV).

case of the SEM, even a resolution below 1 nm can be achieved for the low-landing energy of electrons. [19] Since specimen contamination increases with the increasing electron dose and decreasing landing energy, specimen cleanness is a critical factor in obtaining meaningful data. In this paper we would like to present that the slow electrons can also be used for in-situ samples cleaning, which can lead to elimination of the problem with contamination. An electron-induced in-situ cleaning procedure can be gentle, experimentally convenient, and very effective for a wide range of specimens. Even a small amount of hydrocarbon contamination can severely impact the results obtained with low-energy electrons, as illustrated in Fig. 1A. During the scanning of surfaces by electrons, the image usually darkens because of a carbonaceous layer that is gradually deposited on the top from the adsorbed hydrocarbon precursors and the residue of the cleaning procedures. [20] This effect can be described as electron-stimulated deposition. The surface diffusion of hydrocarbon molecules around the irradiated area serves as a source of additional precursors that are responsible for the even darker frame of the contaminated field of view. On the other hand, the effect of electron-stimulated desorption occurs at the same time, especially at low energies, so the fundamental question arises: which process, deposition, or desorption will dominate – see Fig. 1B.

The cleaning is induced by the so-called electron-stimulated desorption of decomposed residues, which is probably caused by the bond breaking of the contaminants based on multi-electron processes, which follows the electronic excitation induced by the energy of the incident electrons. [21] This effect was also observed in an ultra-high-vacuum device on the in-situ annealed samples, which means that the chemical etching by high reactive OH radicals (generated from the cleaving of water molecules absorbed on the surfaces during irradiation) is not dominated to the observed cleaning effect. However, the cleaning efficiency outside UHV is higher, according to our experience, probably due to the presence of molecules that contain oxygen in the vacuum. Incidentally, the "cleaning" effect caused by electron-beam irradiation mainly by radical etching is very often observed in environmental microscopes working at higher-vacuum condition [22]. Beam irradiation

at a high-electron energy can also lead to surface cleaning. While the irradiation by high-energy electrons in the TEM (60 keV – 300 keV) can break the bonds in adsorbed species and oxygen molecules practically etched the molecules, energy below 1 keV caused electron-stimulated desorption based on multi-electron excitation processes, which can be more gentle processes appropriate for sensitive samples. [23,24] Unfortunately, the electron-beam irradiation cleaning involves many free parameters and very few published papers published have been focused on this problem, especially with regards to low-energy electrons [25,26]. In this paper, we will focus on the slow electron-induced cleaning of the samples in order to open the possibility of observing specimens by ultra-low-energy electrons even outside ultra-high vacuum devices (i.e., standard commercial high-vacuum microscopes). The biggest advantages of this method include availability (i.e., electrons are used both for cleaning and observation), applicability to sensitive samples (i.e., even some structure repairs have been observed on graphene after irradiation [27]), and the process can be sufficiently rapid. Moreover, the influence of electron-impacted energies on the sample quality will be studied in detail by Raman spectroscopy, Energy-dispersive X-ray spectroscopy (EDX), and X-ray photoelectron spectroscopy (XPS).

It should be noted, that other high resolution methods suitable for 2D materials study are scanning tunneling microscopy (STM) and atomic force microscopy (AFM). Nevertheless, both methods are time-consuming and appropriate only for observation of relatively small areas in comparison to SEM.

## 2. Experimentation

The influence of electron-impacted energy on the cleaning (desorption)/contamination (deposition) of free-standing graphene was checked by an ultra-low-voltage STEM measurement (100 eV). Basically, the transmitted signal, after electron treatment, was interpolated in recorded images between sites of an empty hole (100%) and the supporting mesh rung (0%), see Fig. 2.
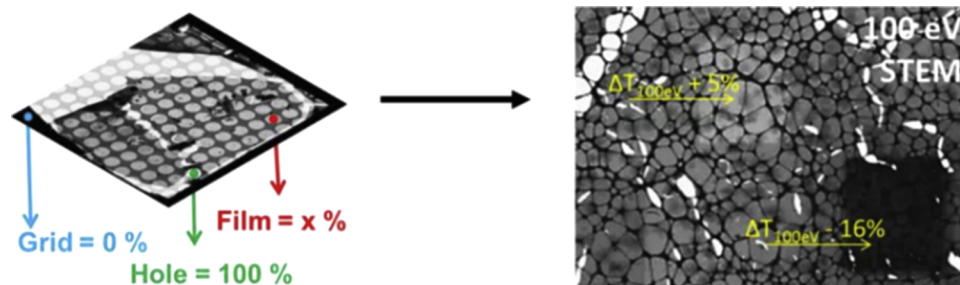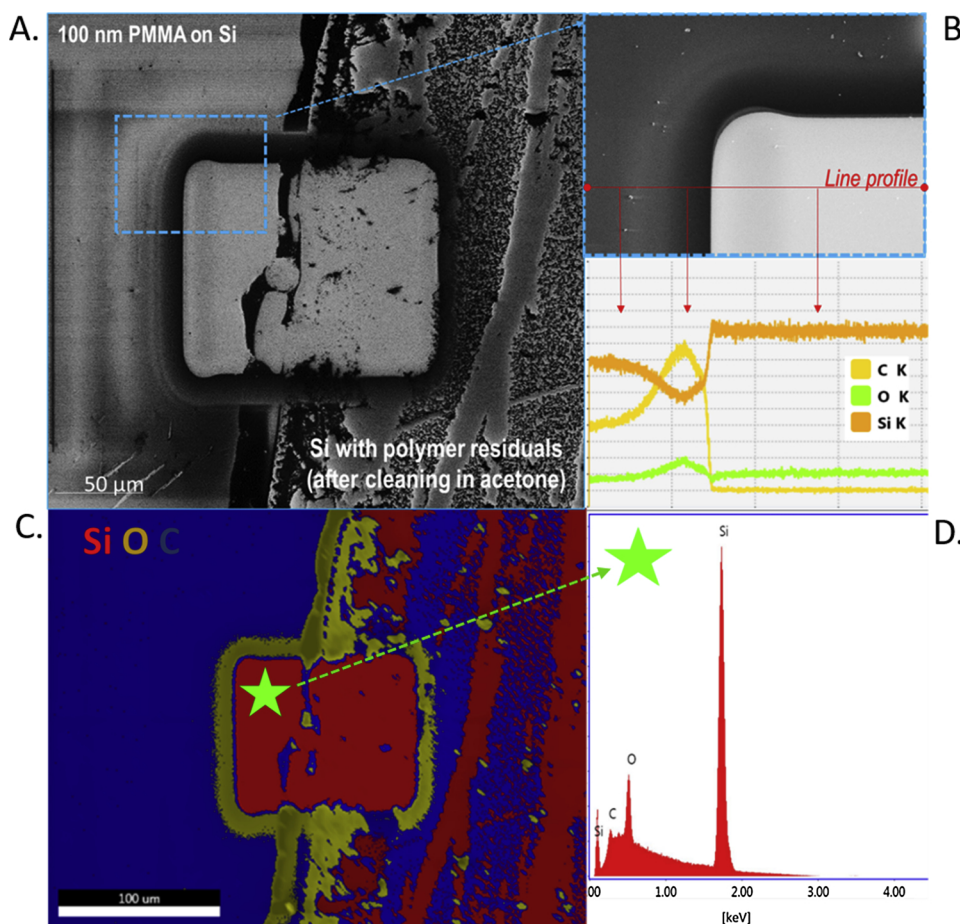


**Fig. 2.** Illustration of the changes in the low-voltage transmissivity of the graphene after electron treatments: cleaning (5% increase)/contamination (16% decrease). The 16-bit image signals were quantified using FIJI software.

**Fig. 3.** The removal of a 100 nm-thick PMMA by slow electrons (500 eV) observed in SEM (1 keV) and analyze by EDX (A. bright square in the middle of SEM image was irradiated by 500 eV electrons, B. EDX line profile of selected elements: C, O and Si on untreated (dark) and treated (bright) parts, C. EDX mapping of selected area (A) and D. EDX point analysis of cleaned area by slow electrons).

## 3. Ultra-low-energy SEM/STEM

The experiments were performed by scanning electron microscopes HR SEM Magellan 400 L (FEI), which are equipped with a beam-deceleration mode, thus enabling us to observe the samples in reflection and transmission modes, practically up to 0 eV. The main characteristic of this method is that the sample holder is held at a high negative bias voltage, so that the electrons leaving the column are decelerated before they reach the sample. [28,29] The microscope works in the standard high-vacuum environment and the pressure in the chamber is about $5*10^{-4}$ Pa. Furthermore, the system is equipped with the Octane Elect EDX system (EDAX), which was used for confirmation of PMMA removal.

## 4. Raman spectroscopy

The influence of electron-beam irradiation on the graphene quality was studied in detail with Raman spectroscopy. Specifically, the quality of the carbon-based materials can easily be tested upon the presence of the D peak in the Raman spectrum. The D band is active on disordered structures in crystalline carbon (e.g., graphene, graphite, nanotubes). The presence of disorders in $sp^2$ hybridization results in resonance in the Raman spectra so this method is one of the most sensitive techniques to characterize disorders in the carbon materials. [30] Raman measurements were made using the 514.5 nm line from an argon ion laser and analyzed using a Jobin Yvon T64000 spectrometer (triple monochromator, resolution ~ 0.5 cm$^{-1}$) equipped with a charge-coupled device. An optical microscope was used to focus the incident light as a spot of about 2 μm in diameter on the sample. The fitting of Lorentzians to the spectra was performed using the MagicPlotStudent program.

## 5. XPS

By deconvolving the C 1s peak we are able to obtain information about the chemical bonds, and the presence of oxygen and nitrogen can be also detected with high accuracy. [31] Moreover, the XPS analyses can be very useful during the exfoliation processes, where the contaminants introduced by chemical etching will be of interest. For analyses, we used the Kratos system - AXIS Supra.

## 6. Ab initio simulations (DFT)

Electron reflection and transmission will be simulated by means of the modern open-source Quantum ESPRESSO (QE) suite for the quantum simulation of materials. [32] The simulations have been done for some layers of graphene. Our results agree with the simulations of Feenstra's group at Carnegie Mellon [33,34] for the Perdew-Burke-Ernzerhof (PBE) exchange correlation functional and with McClain's paper for the Perdew-Zunger (PZ) exchange correlation functional.

## 7. Results

Perhaps the most straightforward expectation connected to the ultra-low-energy microscopy observation is the reduced penetration of electrons into the samples. Naturally, for a true "surface" study, the sample has to be perfectly clean and an in-situ cleaning method is required. Although it is known that contamination molecules can come from the residual atmosphere of the microscope and specimen-borne contaminants (e.g., airborne hydrocarbons, polymer residues, solvent residues) are the main contributors [[35] [36],]. However, the real "surface" studies of material in commercial standard high-vacuum microscopes are not common because of this significant contamination

problem. A range of various specimen-cleaning methods can be applied to selected samples. Typical cleaning methods, such as solvent rinsing, heating, bombarding with ions, and plasma etching, have limitations. We would like to demonstrate that an electron-induced in-situ cleaning procedure can be gentle, experimentally convenient, and very effective for 2D crystals studies, such as graphene.

Graphene was prepared on copper foil with the CVD technique and the transfer was done with a supporting layer of polymethyl methacrylate (PMMA). After the transfer, the PMMA has to be removed precisely, and then we can characterize the samples with selected surface analyses and obtain their unique properties for real applications. For a demonstration of the electron-irradiation power, Fig. 3 shows the removal of a 100 nm-thick PMMA layer and PMMA residues after cleaning in acetone by slow electrons (500 eV, 5 C/cm$^2$), shown as a bright square in the center of the SEM image. The resented point analyses, line profile, and map was obtained by EDX analyses at 5 keV and 1.6 nA.

In Fig. 3, we demonstrate the removal of PMMA induced only by slow electrons. The energy of the impacted electrons was kept at 500 eV and the electron dose was 5 C/cm$^2$. Evidently, the PMMA was precisely removed by the electron irradiation, which was confirmed by EDX line profile and mapping, although the process took hours due to 100 nm thickness of the film. It should be noted that various wet chemical treatments, such as acetone, acetic acid, chloroform, and formamide solution, have been proposed to reduce PMMA. But due to the strong interaction between the PMMA and graphene, its residues were still present on the graphene surface [37].More recently, some new techniques were employed to remove various polymers, including thermal annealing [38], current-induced annealing [39], laser treatment [40], plasma and ozone treatment [41], and a combination of high-energy electron irradiation and a wet chemical treatment [42,43]. However, the previously noticed techniques can easily lead to graphene damage and reproducibility is often problematic.

In the case of PMMA used for graphene transfer, the residues after standard wet cleaning in acetone still has to be removed by ultra-low-energy electron microscopy before the surface analyses. The effectivity of a high dose of slow electrons for the removal of a thick PMMA layer was presented in Fig. 3. We can suppose that for removing polymer residues (after cleaning in acetone), a lower electron dose would be sufficient, which would avoid possible damage of the graphene. In Fig. 4 we demonstrate the electron-beam-induced cleaning of free standing CVD graphene placed on a copper grid covered with lacey carbon. Manifestly, the cleaned part on the sample is presented with the higher transmissivity observed in transmission mode at 100 eV (STEM), and the parts of the treated and the original as-inserted graphene areas are highlighted in green, with respective red slits.

As was already mention in the introduction, the electron-beam irradiation cleaning involves many free parameters, such as electron impacted energy, electron dose, stage bias, etc. From our previous research, one of the most important parameters is electron-landing energy. The influence of electron-landing energy on cleaning/contamination (higher/lower transmissivity observed at 100 eV by STEM) is presented in Table 1. The vacuum was 5.4 * 10$^{-4}$ Pa in the microscope chamber during the experiments and the electron dose was kept at 0.2 C/cm$^2$.

According to Table 1, the chemical etching/desorption process, which means cleaning, is dominant for electron energy below 1 keV and the maximum cleaning efficiency was observed at about 700 eV for the

**Table 1**

Transmitted signal of graphene observed at 100 eV in the standard high-vacuum 5.4 * 10$^{-4}$ Pa after being treated by (20 – 0.3) keV electrons. X- as-inserted sample, red – contamination, green – cleaning.

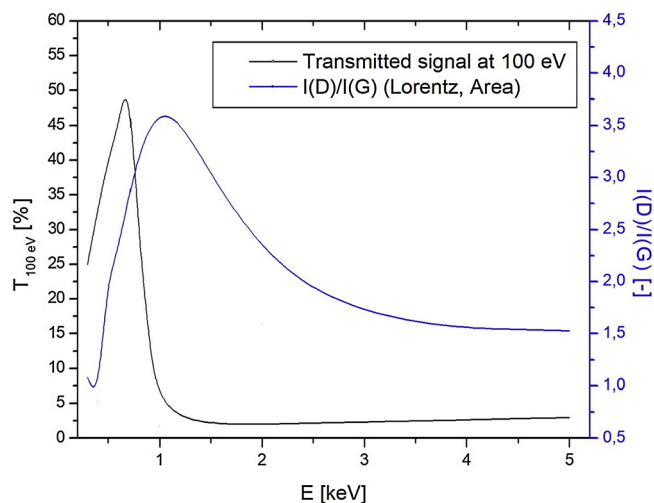| E (keV) | x | 20 | 10 | 5 | 1 | 0.9 | 0.8 | 0.7 | 0.6 | 0.5 | 0.4 | 0.3 |
|---|---|---|---|---|---|---|---|---|---|---|---|---|
| T:100 eV (%) | 8 | 4 | 3 | 2 | 1.8 | 14 | 28 | 53 | 45 | 40 | 33 | 25 |



**Fig. 5.** Transmitted signal observed at 100 eV (inserted graphene: 8%) and the intensity ratio of D and G peaks obtained by Raman spectroscopy (inserted sample: 1.5, 300 eV – 1.12, 500 eV – 2.05, 1000 eV – 3,53, 2000 eV – 2.40, 3000 eV – 1.63, 4000 eV – 1.53 and 5000 eV – 1.50) after irradiation as a function of electron-impacted energy.

following defined conditions: pressure 5*10$^{-4}$ Pa and electron dose 0.2 C/cm$^2$. On the other hand, energy higher than 1 keV leads to sample contamination and a decrease of transmissivity, which is caused by the growing of an amorphous carbon contamination layer on the top. It should be noted that the increase of transmittance can also be caused by the bond breaking of graphene during the irradiation by slow electrons; therefore, the potential irradiation damage has to be controlled. The quality and purity of graphene was checked by Raman spectroscopy and XPS. Fig. 5 shows the intensity ratio for D peak to G peak and the transmitted signal observed at 100 eV after irradiation with various electron energies. The electron dose was kept at 0.2 C/cm$^2$.

The I(D)/I(G) ratio first increases, reaching a maximum of about 1 keV, and then the ratio gradually decreases. These results can be interpreted as the amorphization trajectory, as proposed by Ferrari and Robertson, caused by the creation of an amourphous carbon-based contamination layer on the top during the experiments. [44] Increasing the ratio can also be connected to the transition of crystalline graphene to nanocrystalline graphite, and then decreased when nanocrystalline graphite is transformed into sp$^2$ amorphous carbon. However, the decreasing of the D peak is most probably connected to the lower damage of the sample, which we presented in our previous paper. [24] This means that the 300 eV treatment is more gentle compared to higher energies, although the "cleaning rate" is lower and means that the cleaning time of the samples has to be higher. Murakami et al. also presented the influence of impacted-electron energies and electron dose
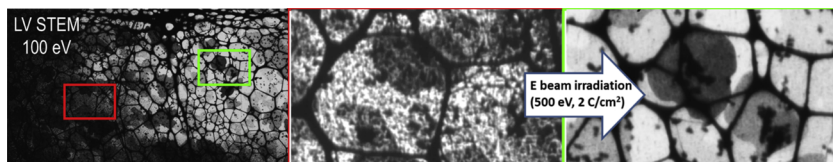


**Fig. 4.** Slow-electron irradiation of multilayered exfoliated CVD graphene: removal of PMMA/acetone/hydrocarbons residues.
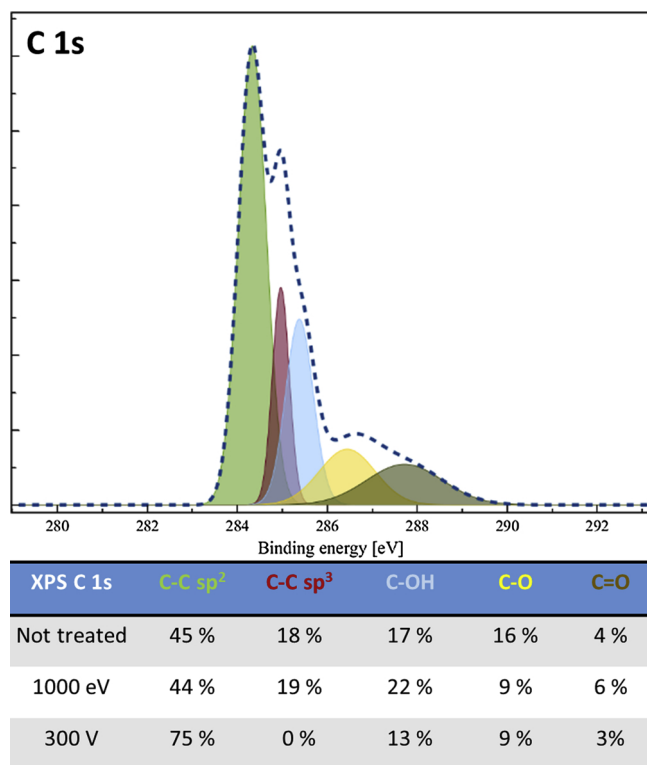
**C 1s**



| XPS C 1s | C-C sp² | C-C sp³ | C-OH | C-O | C=O |
|---|---|---|---|---|---|
| Not treated | 45 % | 18 % | 17 % | 16 % | 4 % |
| 1000 eV | 44 % | 19 % | 22 % | 9 % | 6 % |
| 300 V | 75 % | 0 % | 13 % | 9 % | 3% |

**Fig. 6.** XPS C 1s peak deconvolution corresponding to carbon-carbon sp² hybridization (284.5 eV), carbon sp³ (285.0 eV) hybridization, C—OH (285.4 eV), C—O (286.3 eV), and C=O (287.8 eV).

on the internal strain in graphene structures, which was connected with a G peak shift in the Raman spectra [45]. We also observed the shifts, from $1584.8\,cm^{-1}$ (untreated graphene) to $1574.6\,cm^{-1}$ (treated by 700 eV electrons), while the G peak position was not changed for the 300 eV irradiation electron energy of graphene ($1584.7\ cm^{-1}$). This result may also indicate the more gentle treatment by lower electron energies. The surface chemical properties of the carbon-based films can be analyzed precisely by XPS, via C 1s peak deconvolution, as presented in Fig. 6. The C 1s peak can be deconvoluted into five peaks, which correspond to the carbon-carbon sp² or sp³ hybridization, and contaminants/polymer residues C—OH, C—O, C=O [46].

According to the table presented in Fig. 6, it is evident that 300 eV electron irradiation removes the polymer residues - the spectrum of the graphene before and after being treated by 1000 eV content sp³ hybridization (peak around 285.0 eV), which indicates the amorphous character of the studied graphene area. Indeed, the presence of C—OH, C—O, and C=O was detected for all surfaces, because XPS analyses were done ex-situ. The XPS analyses, together with Raman spectroscopy and low voltage STEM, show the ideal conditions for graphene cleaning by slow electrons. Although the energy level of 700 eV is the most effective, the 300 eV electrons are still sufficient to remove the contaminants without observed damage. For the following presented results obtained by SLEEM and low voltage STEM, the 300 eV electrons were used for sample cleaning.

Unfortunately, contamination is one of the most troublesome problems in modern low-energy-electron microscopy since it induces physical changes in the actual structure of the material being viewed, generally by obscuring fine details. Ultra-low-energy electron observation supported by DFT simulations enable us to count the number of atomic layers, measure the size of the flakes, describe the growth mechanism, and even identify the crystallography phases. [47] Indeed, the samples have to be atomically clean for ultra-low-energy analyses. The precise SLEEM study of the treated CVD graphene on cooper foil by 300 eV electrons is supported by DFT simulations. It is presented in

Fig. 7.

Evidently, the treatment of CVD graphene placed on Cu foil by slow electrons is an appropriate method for the ultra-low-energy electron spectroscopy of graphene outside of UHV devices. Moreover, no additional in-situ cleaning methods are required, and the electron source is used for both cleaning and measurement. The importance of atomic clean surface for ultra-low energy analysis of multi-layered graphene is demonstrated in Fig. 7 A. Evidently, only the presence of absorbed species can be a big problem for surface studies, while the contamination film makes the surface analyses impossible. The cleaning of multi-layered graphene deposited on Cu foil by 300 eV electrons and the obtained spectra (dependence of electron landing energy and signal of reflected electrons) are presented in Fig. 7B. Finally, the obtained experimental results were compared with DFT simulations, which are presented in Fig. 7C. Low-energy electron reflection was simulated by the modern open-source Quantum Espresso (QE) suited for the quantum simulations of materials. The measured oscillations fit very well with simulated data by DFT, which confirms the cleaned efficiency of slow electrons and open the door to precious measurement of surfaces outside the UHV condition. Practically, slow electrons were used just for the removal of the absorbed species on the surface that originated from graphene stay outside the vacuum, such as molecules of water, OH, and hydrocarbons. Nevertheless, the presence of these molecules on the surface makes SLEEM analyses impossible and the trapped species have to be removed precisely, as presented in Fig. 1a.

On the other hand, the PMMA has to be used for the preparation of free-standing graphene, and then for graphene layers to distinguish the PMMA to be removed. According to our previously presented results, 300 eV electrons were used for polymer removing. The results are presented in Fig. 8.

With the decrease of landing energy, an increase in contrast between site differences in graphene thickness was observed. Practically, distinguishing individual layers is possible with electrons impacted with energy below 500 eV. Startlingly, transmissivity that apparently exceeds 100% owing to the contribution of secondary electrons attracted to the grounded detector, created a negative bias that was applied to the sample during the measurements to retard the impacted electrons. Unfortunately, oscillations below 30 eV were not observed in transmission mode, which is probably caused by the presence of various types of damage created during the chemical exfoliation process. However, the differentiation is still possible by the difference in transmissivity below 500 eV due to the ultra-sensitivity of slow electrons. Another reason of oscillation absence in the graph can be 0.5 eV step in electron energy, which is technical limitation of the microscopes and it can lead to missing details. Similar results were obtained with an ultra-high-vacuum microscope by Frank et al. [24] Oscillations in transmission mode were observed by state-of-the-art LEEM, the ev-TEM tool was presented by Geelen et al [48].

## 8. Conclusion

In conclusion, the low-energy-electron irradiation treatment is a powerful technique for the removal of absorbed molecules and even the polymer residues used for 2D material transfer. The influence of electron-impacted energy on cleaning efficiency was studied on free-standing graphene covered by PMMA residues that originated from the exfoliation process. The most powerful electrons had an energy of about 700 eV, but the big impact of graphene quality was observed by Raman spectroscopy. According Raman spectroscopy and XPS, 300 eV electron treatment is more appropriate for graphene cleaning in standard high-vacuum chambers. During 300 eV irradiation, the trapped molecules originated from standing samples outside the vacuum and polymer residues were successfully removed, and graphene quality kept its original state. The cleaning procedure by 300 eV electrons was used for the precise study of graphene by scanning low-energy electron microscopy (SLEEM) and low-voltage STEM in a standard high vacuum, where
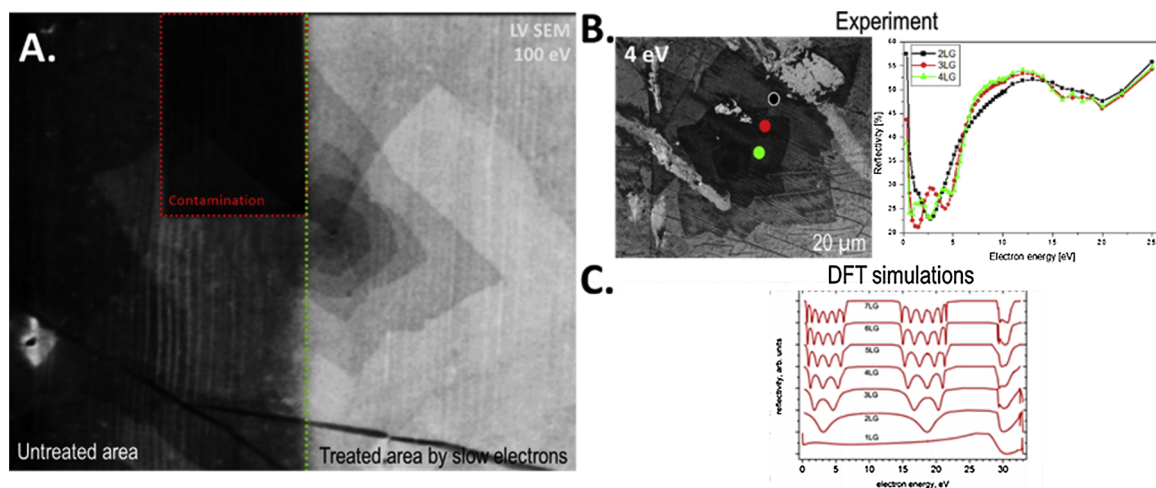
**Fig. 7.** SLEEM study of CVD graphene growth on copper foil (A Multilayered graphene flakes on copper foil: untreated area – treated area by slow electrons – contaminated area by carbon based film after irradiation by higher energy electrons, B Multilayered graphene flakes on copper foil cleaned by slow electrons and measured reflected signal of various thick flakes from 0 eV to 30 eV) supported by DFT simulations (C).
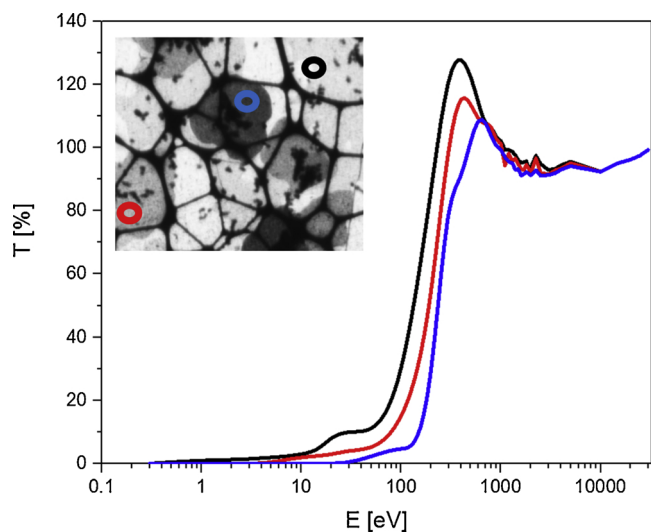


**Fig. 8.** Electron energy dependence of transmissivity from one to several multilayers measured from 30 keV to 0.3 eV.

perfect clean surfaces are required. Distinguished single layers of graphene were presented in both reflection and transmission modes. The experiments were supported by DFT simulations.

The obtained results can be summarized in these following points:

- The electron landing energy about 300 eV is the most appropriate for removing PMMA residues and air born contaminants from exfoliated graphene flakes.
- Higher energies (>300 eV) can cause damage of exfoliated graphene, which was observed by Raman spectroscopy and XPS. Regarding to predicted graphene resistance to inelastic damage, we suppose that the damage is caused by chemical etching by oxygen radicals.
- Graphene layers counting is possible also in the standard high vacuum electron microscopes in both reflection and transmission modes.

## Acknowledgements

## References

[1] M. Taghioskoui, Mater. Today 12 (2009) 34–37.
[2] Y.M. Lin, et al., Science 327 (2010) 662–668.
[3] F. Xia, D.B. Farmer, Y.M. Lin, P. Avouris, Nano Lett. 10 (2010) 715–718.
[4] C.R. Dean, et al., Nature Nanotech. 5 (2010) 722–726.
[5] S.S. Kim, J.H. Jeon, H.I. Kim, C.D. Kee, K.I. Oh, Adv. Funct. Mater. 25 (2015) 3560–3570.
[6] E.P. Randiviir, D.A.C. Brownson, C.A. Banks, Mater. Today 17 (2014) 426–432.
[7] F. Schwierz, Nature Nanotech. 5 (2010) 487–496.
[8] N.O. Weiss, et al., Adv. Mater. 24 (2012) 5782–5825.
[9] J. Liu, Nat. Nanotechnol. 9 (2014) 739–741.
[10] X. Li, et al., Nano Lett. 9 (2009) 4359–4363.
[11] F. Bonaccorso, Z. Sun, T. Hasan, A.C. Ferrari, Nat. Photonics 4 (2010) 611–622.
[12] E.J. Lee, et al., Nature Communication 6 (2015) 6851–6860.
[13] S. Dayou, et al., J. Nanopart. Res. 19 (2017) 336.
[14] M. Chen, et al., Mater. Horiz. 4 (2017) 1054–1063.
[15] B.H. Son, et al., Sci. Rep. 7 (2017) 1–7.
[16] W. Regan, et al., Appl. Phys. Lett. 96 (2010) 113102.
[17] M. Tripathi, et al., Phys. Satutus Solidi RRL (2017) 1700124.
[18] G. Algara-Siller, O. Lehtuinen, A. Turchanin, U. Kaiser, Appl. Phys. Lett. 104 (2014) 153115.
[19] D. Phifer, L. Tuma, T. Vystavel, P. Wandrol, R.J. Young, Micros. Today 17 (2009) 40–49.
[20] M. Issacson, et al., Ultramicroscopy 4 (1979) 193–199.
[21] S. Suzuki, Nanotechnology and Nanomaterials: "Electronic Properties of Carbon Nanotubes", (2011) ISBN 978-953-307-499-3.
[22] M. Toth, et al., J. Appl. Phys. 106 (2009) 034306.
[23] E. Mikmekova, et al., Diam. Relat. Mater. 63 (2016) 136–142.
[24] L. Frank, E. Mikmekova, M. Lejeune, Appl. Surf. Sci. 407 (2017) 105–108.
[25] G.A. Kimmel, T.M. Orlando, P. Cloutier, L. Sanche, J. Phys. Chem. B 101 (1997) 6301–6303.
[26] L. Tao, et al., J. Phys. Chem. C 117 (2013) 10079–10085.
[27] D. Teweldebrhan, A.A. Balandin, Appl. Phys. Lett. 94 (2009) 013101.
[28] L. Frank, et al., Materials 5 (2010) 2731–2756.
[29] I. Mullerova, L. Frank, Modern Research and Educational Topics in Microscopy (2007) 795–804.
[30] A.C. Ferrari, Solid State Commun. 143 (2007) 47–57.
[31] XPS Interpretation of Carbon: https://xpssimplified.com/elements/carbon.php.
[32] P. Giannozzi, et al., J. Phys. Condens. Matter 21 (2009) 395502.
[33] H. Hibino, et al., Phys. Rev. B 77 (2008) 075413.
[34] R.M. Feenstra, et al., Phys. Rev. B 87 (2013) 041406.
[35] J. Hren, et al., Ultramicroscopy 3 (1978) 375–380.
[36] Ch. Soong, P. Woo, D. Hoyle, Micros. Today 20 (2012) 44–48.
[37] A. Pirkle, et al., Appl. Phys. Lett. 99 (2011) 122108.

[38] W. Choi, et al., IEEE Trans. Nanotechnol. 14 (2015) 70–74.
[39] J. Moser, A. Barreiro, A. Bachtold, Appl. Phys. Lett. 91 (2007) 163513.
[40] Y. Jia, et al., Nano-Micro Lett. 8 (2016) 336–346.
[41] Y.D. Lim, ACS Nano 6 (2012) 4410–4417.
[42] M. Her, R. Beams, L. Novotny, Mod. Phys. Lett. B 377 (2013) 1455–1458.
[43] J.W. Suk, et al., Nano Lett. 13 (2013) 1462–1467.

[44] A.C. Ferrari, J. Robertson, Phys. Rev. B 61 (2000) 14095–14107.
[45] K. Murakami, T. Kadowaki, J. Fujita, Appl. Phys. Lett. 102 (2013) 043111.
[46] S.Z. Mortazavi, et al., J. Phys. D Appl. Phys. 46 (2013) 165303.
[47] S. Nie, et al., New J. Phys. 14 (2012) 093028.
[48] D. Geelen, et al., Ultramicroscopy 159 (2015) 482–487.